PHYSICAL REVIEW B **88**, 201305(R) (2013)

High-fidelity biexciton generation in quantum dots by chirped laser pulses

A. Debnath,[1] C. Meier,[1,*] B. Chatel,[1] and T. Amand[2]

[1]*Université de Toulouse, CNRS, LCAR, IRSAMC, 118 Route de Narbonne, 31062 Toulouse, France*

[2]*Université de Toulouse, INSA-CNRS-UPS, LPCNO, 135 Avenue de Rangueil, 31077 Toulouse, France*

(Received 17 July 2013; published 19 November 2013)

We present a detailed theoretical analysis of biexciton state generation in InAs-GaAs quantum dots by strong, chirped laser pulses. Specifically, we derive an accurate analytical expression, which not only provides a clear physical picture of the process, but also allows identifications of laser parameter regimes where efficient biexciton generation should be possible, even at temperatures up to 80 K. The results are confirmed by numerical simulations, in very good agreement with the model proposed. A clear choice of parameters is proposed, which might pave the way towards the optimal design of high-fidelity sources of entangled photon pairs based on individual quantum dots.

DOI: 10.1103/PhysRevB.88.201305 PACS number(s): 73.21.La, 78.67.Hc, 78.47.jm

The efficient generation of biexcitons in semiconductor quantum dots has attracted a lot of interest due to the possibility of developing sources of correlated photons,[1–5] with a wide range of interesting perspectives on various fields such as quantum state teleportation[6,7] in quantum cryptography.[7] However, in order to make practicable polarization entangled sources of photon pairs, the biexciton state needs to be created with a very high quantum yield. The main challenge is that the excitonic states of any quantum dot are not isolated, but coupled to the phonons of the substrate, hampering the coherent one- or two-photon excitation process.

Different protocols have been proposed to overcome these difficulties,[8–14] all of them at temperatures in the range of 4–20 K. Resonant excitation leads to Rabi-type transitions,[15–18] which, however, require perfect control of the interaction strength. More robust schemes are based on adiabatic passage,[8,11–14,19–21] which have also been successfully employed in recent experiments.[22,23] One of the most recent studies[10] concludes that biexciton generation is particularly difficult at high temperatures. Based on a well-established microscopic Hamiltonian[10,13,24] in this Rapid Communication we present an analytical approach, which not only provides a simple physical picture of the process, but, more importantly, allows the identification of parameter regimes where efficient generation of biexcitons should be possible, at temperatures as high as 80 K. The key to this result is that with suitably chosen laser pulses, the phonon interaction can be effectively suppressed, making rapid adiabatic passage successful. The analytical findings are confirmed by numerical simulations, and the pulses are shown to be realistic within the context of optical excitation of quantum dots.

The quantum dynamics of the system under linearly polarized excitation is well described by an effective three-level system taking the ground state (with energy E_0 taken to be zero), the excitonic state (with energy E_X), and the biexciton state (with energy E_B) into account. The chirped Gaussian laser pulse is given by $\mathcal{E} = \frac{1}{2}\mathcal{E}_p e^{-t^2/\tau_p^2} e^{-i(\omega_l t+\alpha t^2)}$. Experimentally, these pulses are obtained by passing a Fourier-transform (FT)-limited pulse of duration τ_0 with a peak field strength $\mathcal{E}_0$ through a pulse-shaping device, which introduces a quadratic phase ϕ''. The pulse parameters of the chirped pulse are then given by[25] $\tau_p = \tau_0(1 + \frac{(2\phi'')^2}{\tau_0^4})$, $\mathcal{E}_p = \mathcal{E}_0\sqrt{\tau_0/\tau_p}$, and $\alpha = (2\phi'')/[\tau_0^4 + (2\phi'')^2]$. Hence a chirped pulse is stretched, and its peak field strength is reduced. However, the pulse energy $\mathcal{P} = \int |\mathcal{E}|^2 dt$ is independent of the chirp parameter.

Using the rotating wave approximation (RWA), the total Hamiltonian (in atomic units) can be written in the basis $|0\rangle, |X\rangle, |B\rangle$ as $H = H_s + \sum_q \omega_q b_q^\dagger b_q + SB$, with the definitions

$$H_s = \begin{pmatrix} \Delta & \frac{\Omega}{2} & 0 \\ \frac{\Omega}{2} & \delta & \frac{\Omega}{2} \\ 0 & \frac{\Omega}{2} & -\Delta \end{pmatrix}, \quad S = \begin{pmatrix} 0 & 0 & 0 \\ 0 & 1 & 0 \\ 0 & 0 & 2 \end{pmatrix}, \tag{1}$$

and $B = \sum_q (g_q b_q^\dagger + g_q^* b_q)$, where g_q is the exciton-phonon coupling amplitude. This model has been successfully used in previous studies on this system.[10,13,24] Here, $2\delta = (E_X - E_0) - (E_B - E_X)$ and $\Delta = \omega_l + 2\alpha t - \frac{1}{2}(E_B - E_0)$. For a two-photon resonance, we have $2\omega_l = E_B - E_0$ and the time-dependent detuning simply becomes $\Delta = 2\alpha t$. The coupling due to the laser interaction is given by $\Omega = \Omega_p e^{-t^2/\tau_p^2}$ with $\Omega_p = \mu_{X0}\mathcal{E}_p$, where we assumed identical dipole strengths $\mu_{X0} = \mu_{BX}$. In terms of Ω, the total interaction strength can be expressed as the pulse area $\theta = \int \Omega(t) dt$.

Within a second order perturbative approach with respect to the quantum dot-phonon interaction, and assuming a thermal equilibrium of the phonon bath at a temperature T, the quantum dynamics of the system, described by the density matrix ρ, is given by the master equation[26–28]

$$\dot{\rho}(t) = L_s\rho + \int_0^t dt' K(t,t')\rho(t'), \tag{2}$$

with $L_s = -i[H_s, \cdot]$ and the memory kernel defined by

$$K(t,t')\rho(t') = i[S, \{ic(t,t')U(t,t')S\rho(t')\} + \{\text{H.c.}\}], \tag{3}$$

using the time-ordered propagator $U(t,t') = \mathcal{T}e^{\int_{t'}^t L_s dt''}$. At this level of description, the phonon dynamics enters via the correlation function $c(t,t') = \int_{-\infty}^{\infty} n_\beta J(\omega) e^{i\omega(t-t')} d\omega$, where $n_\beta = (e^{\beta\omega} - 1)^{-1}$ with $\beta = 1/k_B T$ and the spectral density defined by $J(\omega) = \sum_q |g_q|^2 \delta(\omega - \omega_q)$. For the system under study, the relevant energy range for Rabi splittings is of the order of a few meV, so the interaction of excitons with acoustic phonons is dominant.[17] Thus the spectral density is well approximated by $J(\omega) = A\omega^3 e^{-\omega^2/\omega_c^2}$ with the coupling constant

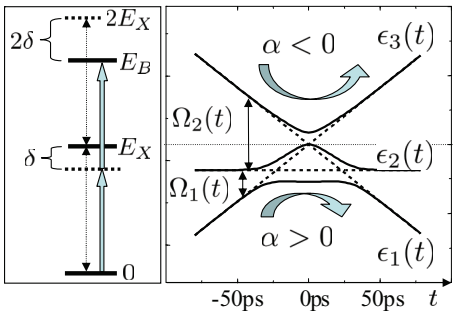

FIG. 1. (Color online) Left: Energy levels of the quantum dot model with ground state $|0\rangle$, exciton state $|X\rangle$, and biexciton state $|B\rangle$. The energy $2\delta = 2E_X - E_B$ represents the biexciton shift. Right: Schematic field dressed eigenstates. The arrows indicate the branches along which adiabatic passage can occur for the different signs of a linear chirp.

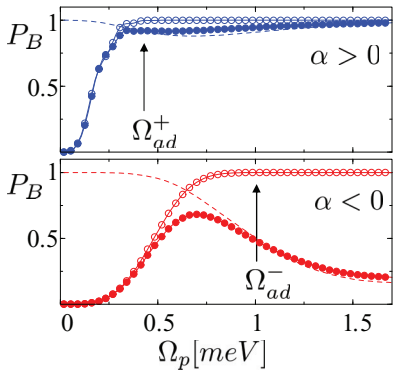

FIG. 2. (Color online) Population of the biexciton state, as a function of peak interaction strength Ω_p, for a laser pulse with $\tau_0 = 1$ ps, $\phi'' = 20$ ps^2 (upper panel), and $\phi'' = -20$ ps^2 (lower panel), resulting in $\tau_p \approx 40$ ps. Solid circles: Numerical solution of Eq. (2). Open circles: Without phonon interaction. Dashed lines: Analytical expression [Eq. (7)]. The biexciton shift is $2\delta = -1.5$ meV and the lattice temperature $T = 4$ K. The highest value shown, $\Omega_p = 1.7$ meV, corresponds to a FT-limited pulse of area $\theta = 9\pi$.

A and a high frequency cutoff induced by the electron-phonon coupling form factor.[17,18] In our previous work, we estimated the coupling constant A from the GaAs bulk parameters,[18,29] and obtained $A = 0.022$ ps^{-2}, which is very close to the measured value reported in Refs. 17 and 18 for similar quantum dots. For the cutoff we used $\omega_c = 0.72$ meV, based on an estimation of the size of our quantum dot. Furthermore, we chose for the biexciton shift $2\delta = -1.5$ meV, as measured in Ref. 22. With these values, very good agreement with experimental results was obtained.[22,24]

The numerical results to be presented are obtained by solving Eq. (2) using the auxiliary density matrix method,[26–28] which is perturbative in the system bath coupling, but takes memory and strong external driving into account. To analyze the field induced dissipative dynamics, in Fig. 1 we plot the time-dependent, instantaneous eigenstates $\epsilon_1(t)$,$\epsilon_2(t)$, and $\epsilon_3(t)$ of the system Hamiltonian $H_s(t)$, numbered according to increasing energy. It is important to notice that depending on the sign of the chirp parameter, the initial state at $t \to -\infty$ is either the upper (for $\alpha < 0$) or the lower adiabatic state (for $\alpha > 0$). In the absence of dissipation, adiabatic passage involves the evolution following the lower or upper instantaneous eigenstates across the coupling, leading to a final biexciton state population $P_B \approx 1$, independent of the sign of α.

To describe nonadiabatic effects and the coupling to the phonons, the pertinent quantities are the time-dependent energy gaps between the adiabatic states, $\Omega_1(t) = \epsilon_2(t) - \epsilon_1(t)$ and $\Omega_2(t) = \epsilon_3(t) - \epsilon_2(t)$. For large enough δ, these gaps bear the fingerprints of three avoided crossings, one at $t = 0$ and two at $t = \pm\delta/(2\alpha)$, either for Ω_1 or Ω_2, depending on the sign of δ.

In the case of a negative δ, corresponding to the quantum dot used in the experiments reported in Ref. 22, $\Omega_1(t)$ is minimal at $t = \pm\delta/(2\alpha)$ with a value $\Omega_1^* \approx \Omega_p \exp(\frac{\delta^2}{4\alpha^2\tau^2})$ and $\Omega_2(t)$ is minimal at $t = 0$ with a value of $\Omega_2^* = \sqrt{\Omega^2/2 + \delta^2/4} - |\delta|/2$ (see Fig. 1).

Assuming pairwise (two-state) transitions, the threshold value $\Omega_{ad}^{\pm}$, such that for $\Omega_p > \Omega_{ad}^{\pm}$ we have adiabatic evolution (and thus 100% transfer efficiency in the isolated case), can be estimated by a simple Landau-Zener analysis,[30] and yields

$$\Omega_{ad}^{+} = \sqrt{8\alpha}\ \exp\left(\frac{\delta^2}{4\alpha^2\tau_p^2}\right) \quad \text{for } \alpha > 0, \tag{4}$$

$$\Omega_{ad}^{-} = 2(8\alpha + 2\sqrt{\alpha}|\delta|)^{1/2} \quad \text{for } \alpha < 0. \tag{5}$$

Since for different signs of the chirp parameter α the passage occurs either on the upper or lower surface, the adiabaticity plateau is reached for different values.

In Fig. 2, we show the final biexciton population P_B after interaction with a strong, chirped laser pulse with $\tau_0 = 1$ ps, $\phi'' = \pm 20$ ps^2, as a function of Ω_p. In each of the panels, we show a full numerical simulation based on Eq. (2) with and without the GaAs matrix phonons, together with the analytical result to be developed below [Eq. (7), dashed line], which is valid in the adiabatic regime, i.e., for $\Omega_p > \Omega_{ad}^{\pm}$. First, without the phonon interaction, we see the adiabatic regime for $\Omega_p > \Omega_{ad}^{\pm}$, where the plateau $P_B = 1$ is reached, confirming the Landau-Zener picture developed above.

The situation is completely different when the phonons are included. The most striking effect is a drastic loss in the transfer efficiency for $\alpha < 0$ (Fig. 2, bottom panel). However, for $\alpha > 0$, the plateau above Ω_{ad}^{+} is approximately maintained. This asymmetry, also found in previous numerical simulations,[10,14] will be explained based on the analytical expression to be detailed below. It is obtained as follows: First, Eq. (2) is transformed into the adiabatic basis, where in the transformation of the memory kernel $K(t,t')$ we have set $\delta = 0$ for simplicity. Neglecting nonadiabatic couplings leads to a set of coupled equations for the density matrix in the adiabatic representation ρ^a. When we further neglect the influence of the coherences ρ_{13}^a onto the populations, the latter are found to obey a closed set of equations. This effective master equation reads

$$\begin{pmatrix} \dot\rho_{11}^a \\ \dot\rho_{22}^a \\ \dot\rho_{33}^a \end{pmatrix} = -f(t) \begin{pmatrix} \gamma_1^- & -\gamma_1^+ & 0 \\ -\gamma_1^- & \gamma_1^+ + \gamma_2^- & -\gamma_2^+ \\ 0 & -\gamma_2^- & \gamma_2^+ \end{pmatrix} \begin{pmatrix} \rho_{11}^a \\ \rho_{22}^a \\ \rho_{33}^a \end{pmatrix}, \tag{6}$$

with $\gamma^{\pm}_{1(2)} = \pi J(\Omega_{1(2)})[\coth(\beta\Omega_{1(2)}/2) \pm 1]$ and $f(t) = \Omega^2/(\Omega^2 + 8\alpha^2 t^2)$. This set of equations is to be solved subject to the initial conditions $\rho^a_{11} = (1 + \alpha/|\alpha|)/2$ and $\rho^a_{33} = (1 - \alpha/|\alpha|)/2$, which yields the biexciton population after the pulse excitation according to $P_B = \rho^a_{11}(t_f)$ for $\alpha > 0$ and $P_B = \rho^a_{33}(t_f)$ for $\alpha < 0$. Using a Gaussian laser pulse $\Omega^2 = \Omega_p^2 \exp(-2\frac{t^2}{\tau_p^2})$, we see that in the case we are interested in, i.e., $\alpha \neq 0$, $f(t)$ represents a finite pulse envelope, which shall be approximated by a simple Gaussian $\exp(-2\frac{t^2}{\tau_r^2})$ with an effective pulse length τ_r chosen in such a way that the full width at half maximum (FWHM) of $f(t)$ is matched.

An analytical solution of this system of equations is still not possible due to the complex time dependence of Ω_1 and Ω_2 entering into $\gamma^{\pm}_{1(2)}$. To proceed, we neglect this time dependence and choose their values at the avoided crossings, i.e., set $\Omega_1 \approx \Omega_1^*$ and $\Omega_2 \approx \Omega_2^*$ in $\gamma^{\pm}_{1(2)}$. Then, Eq. (6) can be solved analytically and we find

$$P_B = \begin{cases} \frac{\gamma_1^+\gamma_2^+}{4\gamma_1\gamma_2 - \gamma_1^+\gamma_2^-} + \frac{\gamma_1^-}{2\bar{\gamma}}(C_{12}^+ e^{-\kappa^+} - C_{12}^- e^{-\kappa^-}) & \text{for } \alpha > 0, \\ \frac{\gamma_1^-\gamma_2^-}{4\gamma_1\gamma_2 - \gamma_1^+\gamma_2^-} + \frac{\gamma_2^+}{2\bar{\gamma}}(C_{21}^+ e^{-\kappa^+} - C_{21}^- e^{-\kappa^-}) & \text{for } \alpha < 0, \end{cases} \tag{7}$$

where we have defined $C^{\pm}_{ij} = (\gamma_i - \gamma_j \pm \bar{\gamma})/(\gamma_i + \gamma_j \pm \bar{\gamma})$ with $\gamma_{1(2)} = \pi J(\Omega^*_{1(2)}) \coth(\beta\Omega^*_{1(2)}/2)$ and $\bar{\gamma} = \sqrt{\gamma_1^+\gamma_2^- + (\gamma_2 - \gamma_1)^2}$. The exponents are given by $\kappa^{\pm} = \frac{\pi}{8}(\gamma_1 + \gamma_2 \pm \bar{\gamma})\tau_r$. These analytical expressions are depicted as dashed lines in Fig. 2, valid in the adiabatic regime $\Omega_p > \Omega^{\pm}_{ad}$. The above-mentioned asymmetry with respect to α can be rationalized in terms of our analytical expression. Using the low temperature approximations $\gamma^-_{1(2)} \approx 0, \gamma^+_{1(2)} \approx 2\gamma_{1(2)}$ we deduce

$$P_B = \begin{cases} 1 & \text{for } \alpha > 0, \\ e^{-\sqrt{\frac{\pi}{2}}\tau_r\gamma_2} & \text{for } \alpha < 0, \end{cases} \tag{8}$$

from Eq. (7). Hence the physical picture that arises is the following: For $\alpha < 0$ the transfer occurs on the upper surface, and the coupling to the phonons leads to relaxation to the other surfaces, thus diminishing the transfer efficiency. This is reflected in Eq. (8), where for $\alpha < 0$ we find a Landau-Zener-type expression which involves Ω_2^*, i.e., the energy gap for the upper avoided crossing (see Fig. 1). For $\alpha > 0$, however, the transition proceeds on the lower adiabatic surface, and a phonon induced transfer to the other states would require phonon absorption, which is strongly suppressed in the limit of low temperatures.

Even though for lower temperatures $P_B \approx 1$ is possible by choosing the correct sign of the chirp parameter, a significant drop in P_B is found for higher temperatures: Figure 3 shows the biexciton population for different temperatures, up to 80 K, using the same laser parameters as in Fig. 2. Again, we see a very good agreement between the full numerical solution based on Eq. (2) and the analytical expression Eq. (7) (dashed line), which is valid for $\Omega_p > \Omega^{\pm}_{ad}$. The drastic drop in P_B at $T = 80$ K constitutes a major drawback from a technological point of view, since cryogenic technical issues are much harder to solve below liquid nitrogen temperature.

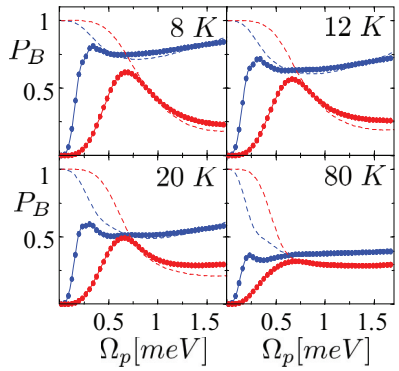

FIG. 3. (Color online) Biexciton population as a function of peak interaction strength Ω_p for different temperatures, as indicated, for a pulse with $\tau_0 = 1$ ps and $\phi'' = \pm 20$ ps^2. A drastic loss of transfer efficiency is found for higher temperatures, predicted by the analytical model, which is valid in the adiabatic regime.

Based on our analytical approach, Eq. (7), we can establish parameter regimes where $P_B \approx 1$ is possible even at this high temperature. In the limit of high temperatures, we can approximate $\gamma^+_{1(2)} \approx \gamma^-_{1(2)} \approx \gamma_{1(2)}$, leading to

$$P_B = \begin{cases} \frac{1}{3} + \left(\frac{1}{3} + R_{12}\right) e^{-\kappa^+} + \left(\frac{1}{3} - R_{12}\right) e^{-\kappa^-} & \text{for } \alpha > 0, \\ \frac{1}{3} + \left(\frac{1}{3} + R_{21}\right) e^{-\kappa^+} + \left(\frac{1}{3} - R_{21}\right) e^{-\kappa^-} & \text{for } \alpha < 0, \end{cases} \tag{9}$$

with $R_{ij} = (\gamma_i - 2\gamma_j)/(6\bar{\gamma})$. Hence, for $P_B \approx 1$ we require $\kappa^+ \approx \kappa^-$, which implies $\kappa^{\pm} \approx 0$ that can be achieved by $J(\Omega^*_{1(2)}) \approx 0$. This condition simply states that the gaps at the avoided crossings depicted in Fig. 2 should be much larger than the cutoff frequency of the spectral density. In this case, the electronic motion becomes so fast that the phonon dynamics is effectively decoupled. This phenomena has also been predicted with unchirped, resonant pulses, leading to Rabi-type transitions. Here, when for strong coupling the Rabi frequency exceeds the cutoff ω_c, an undamping of the Rabi oscillation has been obtained, indicating a decreased coupling to the phonons.[19,31–33] In our case, this can be achieved when $\Omega^*_{1(2)} \gg \omega_c$. For the spectral density considered in this work, we have chosen $\Omega^*_{1(2)} > 4\omega_c$, leading to threshold values defined as *dynamical decoupling*,

$$\Omega^+_{dc} = 4\omega_c \exp\left(\frac{\delta^2}{4\alpha^2\tau_p^2}\right) \quad \text{for } \alpha > 0, \tag{10}$$

$$\Omega^-_{dc} = 4\sqrt{2}\,\omega_c \quad \text{for } \alpha < 0. \tag{11}$$

Since the separation of the avoided crossing increases with peak intensity, intense pulses are required. Furthermore, for a laser with a given intensity, a shorter and only weakly chirped pulse favors the high temperature biexciton generation. Figure 4 shows the biexciton population for a $\tau_0 = 350$ fs laser pulse and a chirp parameter of $\phi'' = \pm 0.5$ ps^2, leading to $\tau_p = 2.8$ ps. Here, the highest intensity considered corresponds to a pulse area of the FT-limited pulse of area 5.2π. One sees that for both chirp signs, $P_B \approx 1$ is possible, even at a temperature of 80 K. For the values chosen, the different threshold values for adiabatic evolution and dynamic decoupling are indicated as arrows for both chirp signs.

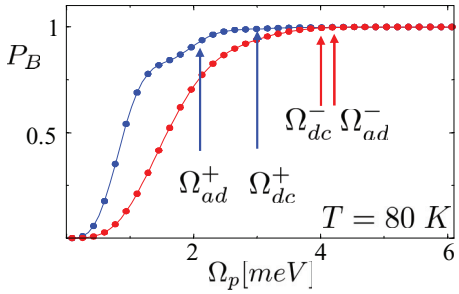

FIG. 4. (Color online) Biexciton population for a short ($\tau_0 = 350$ fs) and only weakly chirped pulse (blue: $\phi'' = 0.5$ ps^2; red: $\phi'' = -0.5$ ps^2; leading to $\tau_p = 2.8$ ps), calculated by a numerical solution of Eq. (2). $P_B \approx 1$ is achieved when both $\Omega_p > \Omega_{ad}^{\pm}$ and $\Omega_p > \Omega_{dc}^{\pm}$ are fulfilled. The highest shown value, $\Omega_p = 6$ meV, corresponds to a FT-limited pulse of area $\theta = 5.2\pi$.

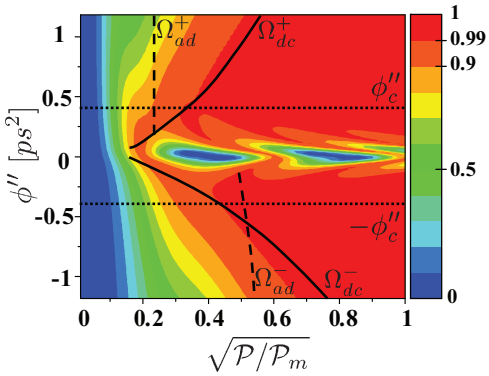

FIG. 5. (Color online) Biexciton population as a function of intensity and chirp parameter, based on a FT-limited pulse with $\tau_0 = 350$ fs and a maximum intensity corresponding to $\theta = 7\pi$, at a temperature of 80 K. The lines correspond to the threshold values [Eqs. (4), (5), (10), and (11)], which, together with $|\phi''| > \pi\tau_0^2$, define regions in parameter space where $P_B \approx 1$ could be realized (red areas correspond to $P_B > 0.99$).

Finally, in Fig. 5 we plot a map of P_B for $\tau_0 = 350$ fs, obtained by the full numerical solution based on Eq. (3) using $T = 80$ K and $2\delta = -1.5$ meV. The intensity is given with reference to $\mathcal{P}_m$, which corresponds to a FT-limited pulse of $\theta = 7\pi$. In this figure, we have indicated the condition for adiabaticity [Eqs. (4) and (5)] and for dynamical decoupling [Eqs. (10) and (11)]. Close to $\alpha \approx 0$, we find the typical coherent population transfer showing a generalized Rabi flopping. To access the adiabatic regime, the absolute value of the chirp parameter needs to be larger than a minimal value ϕ_c''.[34] In Refs. 24 and 34, a value of $\phi_c = \pi\tau_0^2$ is estimated, which coincides with our finding here. Taking all these conditions together, we can identify regions where a plateau of $P_B \approx 1$ is reached. We further checked that the adiabatic passage for biexciton preparation is also robust with respect to variations of δ from dot to dot.[35]

These considerations are important for the realization of high efficiency correlated photon sources. First, the exciton generation is deterministic, occurring at well-defined instants, an advantage with respect to nonresonantly excited sources.[3,5,6,36,37] The quasiresonant character of the excitation prevents the generation of fluctuating charges in the vicinity of the quantum dots,[38] which should lead to longer correlation times and thus better photon indistinguishability.[36,37] Furthermore, electron-hole pair recapture by the dot[3,4] would be reduced, thus improving the quantum correlation between the two emitted photons from the biexciton cascade, hence the overall efficiency of the device.

In conclusion, we have developed a theory of rapid adiabatic passage for the preparation of a biexciton state in a single quantum dot coupled to a phonon bath. In the adiabatic limit, we have derived an accurate analytical expression for the final biexciton population, which makes the physics of the process transparent, in particular, the asymmetry between positive and negative chirp rates. The analytical approach also allows to identify parameter regimes, where $P_B \sim 1$ at $T = 80$ K is possible, proposing an experimental strategy for biexciton generation at temperatures accessible by liquid nitrogen. These findings are very promising in view of the optimal design of robust and efficient sources of correlated photons.

Support by the ITN networks "SPIN-OPTRONICS" and "FASTQUAST" and by the ANR "PROCONTROL" is gratefully acknowledged, as well as the computational resources provided by CICT (Toulouse).

*Corresponding author: chris@irsamc.ups-tlse.fr

[1] E. Moreau, I. Robert, L. Manin, V. Thierry-Mieg, J. M. Gérard, and I. Abram, Phys. Rev. Lett. **87**, 183601 (2001).

[2] R. Stevenson, R. J. Young, P. Atkinson, K. Cooper, D. A. Ritchie, and A. J. Shields, Nature (London) **439**, 179 (2006).

[3] A. Dousse, J. Suffczynski, A. Beveratos, O. Krebs, A. Lemaitre, I. Sagnes, J. Bloch, P. Voisin, and P. Senellart, Nature (London) **466**, 217 (2010).

[4] R. M. Stevenson, A. J. Hudson, A. J. Bennett, R. J. Young, C. A. Nicoll, D. A. Ritchie, and A. J. Shields, Phys. Rev. Lett. **101**, 170501 (2008).

[5] T. Kuroda, T. Mano, N. Ha, N. Nakajima, H. Kumano, B. Urbaszek, M. Jo, M. Abbarchi, Y. Sakuma, K. Sakoda, I. Suemune, X. Marie, and T. Amand, Phys. Rev. B **88**, 041306(R) (2013).

[6] J. Nilsson, R. M. Stevenson, K. H. Chan, J. Skiba-Szymanska, M. Lucamarini, M. B. Ward, A. J. Benett, C. L. Stater, I. Farrer, D. A. Richie, and A. J. Shields, Nat. Photonics **7**, 311 (2013).

[7] P. Kok, W. J. Munro, K. Nemoto, T. C. Ralph, J. P. Dowling, and G. J. Milburn, Rev. Mod. Phys. **79**, 135 (2007).

[8] H. Y. Hui and R. B. Liu, Phys. Rev. B **78**, 155315 (2008).

[9] D. Gerbasi, G. D. Scholes, and P. Brumer, Phys. Rev. B **82**, 125321 (2010).

[10] M. Glässl, A. M. Barth, K. Gawarecki, P. Machnikowski, M. D. Croitoru, S. Lüker, D. E. Reiter, T. Kuhn, and V. M. Axt, Phys. Rev. B **87**, 085303 (2013).

[11] M. Glässl, A. M. Barth, and V. M. Axt, Phys. Rev. Lett. **110**, 147401 (2013).

[12]G. Bensky, S. V. Nair, H. E. Ruda, S. Dasgupta, G. Kurizki, and P. Brumer, J. Phys. B **46**, 055503 (2013).
[13]S. Lüker, K. Gawarecki, D. E. Reiter, A. Grodecka-Grad, V. M. Axt, P. Machnikowski, and T. Kuhn, Phys. Rev. B **85**, 121302 (2012).
[14]K. Gawarecki, S. Lüker, D. E. Reiter, T. Kuhn, M. Glässl, V. M. Axt, A. Grodecka-Grad, and P. Machnikowski, Phys. Rev. B **86**, 235301 (2012).
[15]A. Krügel, V. M. Axt, T. Kuhn, P. Machnikowski, and A. Vagov, Appl. Phys. B **81**, 897 (2005).
[16]S. Stufler, P. Machnikowski, P. Ester, M. Bichler, V. M. Axt, T. Kuhn, and A. Zrenner, Phys. Rev. B **73**, 125304 (2006).
[17]A. J. Ramsay, T. M. Godden, S. J. Boyle, E. M. Gauger, A. Nazir, B. W. Lovett, A. M. Fox, and M. S. Skolnick, Phys. Rev. Lett. **105**, 177402 (2010).
[18]A. J. Ramsay, A. V. Gopal, E. M. Gauger, A. Nazir, B. W. Lovett, A. M. Fox, and M. S. Skolnick, Phys. Rev. Lett. **104**, 017402 (2010).
[19]D. E. Reiter, S. Lüker, K. Gawarecki, A. Grodecka-Grad, P. Machnikowski, V. M. Axt, and T. Kuhn, Acta Phys. Pol. A **122**, 1065 (2012).
[20]E. R. Schmidgall, P. R. Eastham, and R. T. Phillips, Phys. Rev. B **81**, 195306 (2010).
[21]P. R. Eastham, A. O. Spracklen, and J. Keeling, Phys. Rev. B **87**, 195306 (2013).
[22]C.-M. Simon, T. Belhadj, B. Chatel, T. Amand, P. Renucci, A. Lemaitre, O. Krebs, P. A. Dalgarno, R. J. Warburton, X. Marie, and B. Urbaszek, Phys. Rev. Lett. **106**, 166801 (2011).
[23]Y. Wu, I. M. Piper, M. Ediger, P. Brereton, E. R. Schmidgall, P. R. Eastham, M. Hugues, M. Hopkinson, and R. T. Phillips, Phys. Rev. Lett. **106**, 067401 (2011).
[24]A. Debnath, C. Meier, B. Chatel, and T. Amand, Phys. Rev. B **86**, 161304(R) (2012).
[25]B. Chatel, J. Degert, and B. Girard, Phys. Rev. A **70**, 053414 (2004).
[26]C. Meier and D. J. Tannor, J. Chem. Phys. **111**, 3365 (1999).
[27]U. Kleinekathöfer, J. Chem. Phys. **121**, 2505 (2004).
[28]A. Pomyalov, C. Meier, and D. Tannor, Chem. Phys. **370**, 98 (2010).
[29]I. Vurgaftman, J. R. Meyer, and L. R. Ram-Mohan, J. Appl. Phys. **89**, 5815 (2001).
[30]D. J. Tannor, *Quantum Mechanics: A Time Dependent Perspective* (University Science Books, Sausalito, CA, 2007).
[31]A. Vagov, M. D. Croitoru, V. M. Axt, T. Kuhn, and F. M. Peeters, Phys. Status Solidi B **243**, 2233 (2006).
[32]A. Vagov, M. D. Croitoru, V. M. Axt, T. Kuhn, and F. M. Peeters, Phys. Rev. Lett. **98**, 227403 (2007).
[33]M. Glässl, M. D. Croitoru, A. Vagov, V. M. Axt, and T. Kuhn, Phys. Rev. B **84**, 125304 (2011).
[34]V. Malinovsky and J. Krause, Eur. Phys. J. D **14**, 147 (2001).
[35]See Supplemental Material at http://link.aps.org/supplemental/10.1103/PhysRevB.88.201305 for a numerical evaluation based on Eq. (2) of the biexciton generation robustness corresponding to different values of the biexciton shift.
[36]R. B. Patel, A. J. Bennett, K. Cooper, P. Atkinson, C. A. Nicoll, D. A. Ritchie, and A. J. Shields, Phys. Rev. Lett. **100**, 207405 (2008).
[37]A. J. Bennett, R. B. Patel, C. A. Nicoll, D. A. Ritchie, and A. J. Shields, Nat. Phys. **5**, 715 (2009).
[38]A. Berthelot, I. Favero, G. Cassabois, C. Voisin, C. Delalande, P. Rossignol, R. Ferreira, and J.-M. Gérard, Nat. Phys. **2**, 759 (2006).